Edinburgh Research Explorer

Co-combustion, co-densification, and pollutant emission characteristics of charcoal-based briquettes prepared using bio-tar as a binder

1   **Co-combustion, co-densification, and pollutant emission**

2   **characteristics of charcoal-based briquettes prepared using bio-tar as**

3   **a binder**

4   Hongbin Cong[a], Zonglu Yao[b], Ondřej Mašek[c], Haibo Meng[a], Chenxu Sheng[a,d],

5   Yunong Wu[a], Lixin Zhao[b,*]

6   [a]*Academy of Agricultural Planning and Engineering, Key Laboratory of Energy*

7   *Resource Utilization from Agriculture Residue, Ministry of Agriculture and Rural*

8   *Affairs, Beijing 100125, China*

9   [b]*Institute of Environment and Sustainable Development in Agriculture, CAAS, Beijing*

10   *100081, China*

11   [c] *UK Biochar Research Centre, School of Geosciences, University of Edinburgh,*

12   *King's Buildings, Edinburgh EH93FF, UK*

13   [d] *Heilongjiang Bayi Agricultural University, Daqing 163319, China*

14

15   **Corresponding author:** Lixin Zhao **E-mail:** zhaolixin5092@163.com

16

17

18

19

20

21

ABSTRACT: In this study, charcoal-based briquettes prepared using bio-tar as a binder are proposed as a substitute for conventional coal in rural China; furthermore, the fuel properties of the blends of charcoal, semi-coke, and bio-tar and the co-densification and pollutant emission characteristics of charcoal-based briquettes are investigated. The addition of charcoal improved the heating value and combustion index; however, the addition of a small amount of bio-tar did not have any significant effect on the fuel properties of the charcoal and semi-coke blend. The blending of charcoal and semi-coke with a mass ratio of 1:1 increased the integrated combustion characteristics from 7.73×10^{-12} (only semi-coke) to 16.92×10^{-12} $K^{-3}min^{-2}$. Results of the co-densification experiments suggest that the bio-tar effectively improved the physical stability of charcoal-based briquette. By increasing the addition of bio-tar from 0 to 9 wt% at the densification temperature of 20 °C, the strength compaction and drop resistance increased by 8.6% and 13.9%, respectively. Increasing the densification temperature from 20 to 50 °C resulted in negative effects on mechanical strength. Pollutant emissions were observed during the ignition, stable combustion, and burnout phases of the stove. The bio-tar addition had distinct negative influences, increasing the total suspended particle and VOC emissions, which could be effectively weakened or eliminated by adding 3 wt% of hydrated lime. Herein, the applied chain and technical chain of charcoal-based briquettes are summarized. The study provides technical support for the industrial application of charcoal-based briquettes in rural China, with replication potential elsewhere.

1. Introduction

Heating in rural area of north China faces prominent problems such as underdeveloped heating infrastructure, low energy efficiency, and high pollutant emission [1]. The annual consumption of heating coal is approximately 400 million tons of standard coal in China, of which approximately 200 million tons is accounted by scattered burning in rural areas [2]. The use of conventional coal with poor quality plays a crucial role in the formation of haze. Therefore, the "substituting conventional coal" project was proposed by the government [3]. To overcome this issue, an effective strategy is to partially replace or improve the conventional coal, as it is difficult to completely replace coal in short term.

Semi-coke and charcoal are cleaner than raw coal, and are therefore encouraged for use as heating fuel in China [4][5]. Semi-coke and charcoal are obtained from bituminous raw coal and tree branches, respectively, by using the slow pyrolysis technology [6]. Given the relationship between mass density, energy density, and mechanical strength, the use of densified fuels with raw solid fuels is critical [7][8]. The semi-coke and charcoal are generally densified individually or codensified with other solid fuels into briquettes to improve the fuel properties [9][10]. Small amounts of starch, sodium nitrate, limestone, borax, and sawdust are generally added to briquettes for improving ignition, promoting steady burning, and to achieve efficient

64   manufacturing [11]. A honeycomb briquette was developed from a blend of semi-coke

65   and corn stover char, and the value-chain model analysis of the new fuel suggests that

66   it has promising application prospects as a heating fuel in rural China [12]. However,

67   difficulties in handling and using bio-tar presented a severe problem to the biomass

68   pyrolysis project. Bio-tar is a complex organic mixture of condensable or non-

69   condensable hydrocarbons comprising 1- to 5-ring aromatic compounds along with

70   other oxygen-containing hydrocarbons and polycyclic aromatic hydrocarbons; it poses

71   a severe risk of contamination if discarded [13]. In rural China, in addition to crop

72   straws, many wooden materials are collected from orchards. Developing charcoal-

73   based briquettes using bio-tar as a binder is an effective way to solve the

74   abovementioned problem. Therefore, it is necessary to systematically investigate the

75   fuel properties, co-densification characteristics, and pollutant emission characteristics

76   of the blends of charcoal, semi-coke, and bio-tar.

77   From the viewpoint of fuel properties, such as alkali and alkaline earth metal

78   content, bulk density, and heating value [14], charcoal, semi-coke, and bio-tar might

79   have some complementary effects, which should be determined. In particular, the co-

80   combustion characteristics of several kinds of blends, such as straw, municipal solid

81   waste, raw coal, sludge, and oil shale, have been studied [15][16]; however, a

82   considerable knowledge gap remains from the viewpoint of blends of charcoal, semi-

83   coke, and bio-tar. From the viewpoint of co-densification, bio-tar is an effective

84   lubricant and binder for the densification process owing to its high viscosity [10][17].

85   Although several studies have investigated the co-densification characteristics of

86   blends of biomass, char, or raw coal with starch, clay, polymer plastic, or wood fiber

87   as a binder [18][19], the co-densification characteristics of charcoal and semi-coke

88   using bio-tar as a binder have rarely been investigated. In particular, most studies have

89   focused on the material ratio, pressure, moisture content, and particle size in co-

90   densification experiments [18][19][20]. The viscosity of bio-tar can be reduced and its

91   fluidity can be improved by properly increasing its temperature (35–50 °C). In this

92   study, the densification temperature was also considered as an influencing factor. The

93   optimized co-densification condition of bio-tar addition ratio and co-densification

94   temperature should be determined. Moreover, information pertaining to the flue

95   emission from combustion of charcoal-based briquettes is limited. The addition of bio-

96   tar to briquettes might affect pollutant emissions, especially particulate matter (PM)

97   and volatile organic compound (VOC) emissions [21]. Therefore, the pollutant

98   emission from combustion of charcoal-based briquettes, when bio-tar is used as a binder,

99   should also be considered.

100   This study primarily aims to investigate the fuel properties, co-densification

101   characteristics, and pollutant emission characteristics of blends of charcoal, semi-coke,

102   and bio-tar. Herein, we aim to establish a method for using the bio-tar produced by

103   biomass pyrolysis projects; furthermore, we aim to report results that are beneficial for

104   developing a new clean fuel suitable for heating in rural China. This paper also

105   summarizes the applied chain and technical chain of the charcoal-based briquettes to

106 provide basic support for industrial application of the charcoal-based briquettes using

107 bio-tar as a binder in rural China.

108 **2. Materials and methods**

109 *2.1 Materials*

110 The raw materials primarily included charcoal, semi-coke, and bio-tar. Charcoal from

111 tree branches was produced at a pyrolysis temperature of 550–600 °C and residence

112 time of 30–35 min in the Qiannanyu Biomass Pyrolysis Demonstration Project of

113 Hebei Province [22]. Semi-coke was produced via low-temperature pyrolysis of

114 volatile bituminous coal from Shenmu County, Shaanxi Province. The bio-tar was

115 also collected from the Qiannanyu Biomass Pyrolysis Demonstration Project as a by-

116 product of tree branch pyrolysis at the abovementioned conditions. Heating values

117 were measured using a bomb calorimeter (LECO AC-300) following the adiabatic

118 method according to the China National Standard (GB T 213 2008) [23]. Ultimate

119 analysis (carbon, hydrogen, nitrogen, and sulfur) was performed using a Vario ELIII

120 Elemental Analyzer according to ASTM D5373 and ASTM D4239 [24][25]. The

121 metal element contents were determined by inductively coupled plasma mass

122 spectrometry (Thermo Fisher Scientific) according to the AOAC official method

123 975.03.

124 *2.2 Experimental facility*

125   *2.2.1 Testing instrument setup*

126   Thermogravimetric analyzer (DTG-6A) manufactured by Shimadzu Corporation

was used to analyze the combustion characteristics. The reactor had a diameter of 60

mm, and the reaction atmosphere was canned air. The initial test temperatures were set

at 20 °C, which were increased to 1 000 °C at a heating rate of 10 °C/min; air flow rate

was 100 mL/min. Single and blended samples were milled to less than 0.15 mm, and

approximately 10 mg sample was used for each test.

Total suspended particles (TSP) were collected using an electrical low-pressure

impactor (Dekati ELPI+) manufactured by DEKATI Ltd., which can collect particles

from 6 nm to 10 μm in 14 size fractions. The mass size and number size distributions

of TSP were estimated using ELPI software V12.0. To ensure that the collected PM

was kept below saturation, flue gas was diluted 64 times using two Dekati diluters.

Flue gas analyzer (ECOM-J2KN) manufactured by RBR was used to test the NO_X

and SO_2 emissions. In response to the ignition, stable combustion, and burnout phases

of stove running, flue gases were tested four times, once every 3 min. The results were

converted from ppm to mg/Nm^3.

2.2.2 Densification platform and test setup

Densification experiments were conducted using a customized die with

cooperation of a universal testing machine (Fig. 1a). The die mainly comprised a die

piston, die sleeve, and heating jacket. The die sleeve had an inner diameter of 60 mm,

outer height of 120 mm, and a cylinder with diameter of 25 mm on the central axis. A

heating jacket connected to temperature control system was installed on the outside of

die sleeve to heat the raw materials.

148   Particle size is a key factor influencing the densification performance [20]. To

149   ensure consistent particle size distribution of raw materials for all the densification

150   experiments, the semi-coke and charcoal were individually milled on a disintegrating

151   mill once for all. The particle size distributions are shown in Fig. S1. Bio-tar was added

152   to the blends of charcoal and semi-coke using a pipette according to the experimental

153   design. During this process, the bio-tar was heated to approximately 50 °C in a water

154   bath to enhance its fluidity for pumping with pipette. Under experimental conditions

155   with heating, the raw material was filled into the die sleeve, and temperature of the

156   heating jacket was increased to the desired level and held for 5 min. Finally, the die

157   piston started to move for densification. Once the die piston reached desired pressure

158   of 10 kN, it was maintained for 20 s for all the densification experiments.
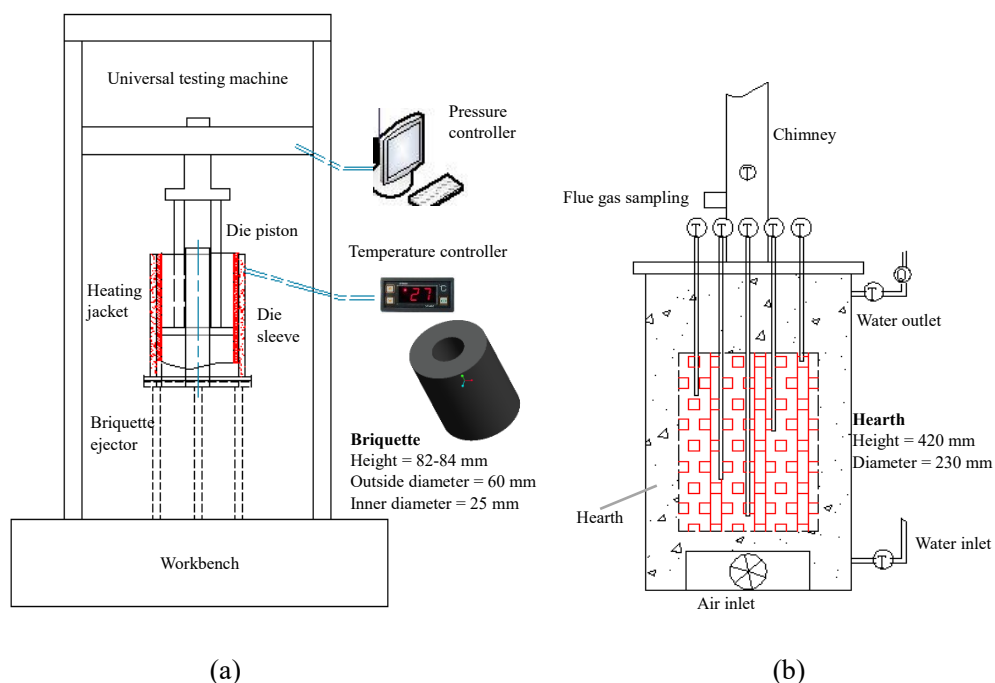
159

160   (a)   (b)

161   Fig. 1. Schematic of the (a) densification testing platform and (b) emission testing

162   platform.

2.2.3 Pollutant emission platform and test setup

164   Herein, an NF9C household heating stove was used. The hearth height, outer length

165   × width, and inner diameter of the stove are 650, 480 × 480, and 230 mm, respectively

166   (Fig. 1b). It features an air inlet with a diameter of 60 mm near the bottom. Air inlet

167   was set up with an open ratio of 100% during pollutant emission tests, and the flue gas

168   was sampled or real-time tested on ignition, stable combustion, and burnout phases.

169   Charcoal-based briquettes with a height of 83–85 mm, outer diameter of 60 mm, and

170   hole with a diameter of 25 mm were used herein. For contrast analysis, three kinds of

171   briquettes were used in the emission experiments.

2.3 Determination of co-combustion, co-densification and pollutant emission

characteristics

174   Combustion characteristics can be evaluated using several combustion parameters,

175   such as ignition temperature, burnout temperature, burnout characteristics, and

176   integrated combustion characteristics [27]. Burnout index C_b (10^{-4}/min) was used to

177   characterize the burnout characteristics of samples; herein, large values represent better

178   burnout characteristics.

$$C_b = \frac{f_1 \cdot f_2}{t_0}, \qquad (1)$$

180   where f_1 (%) is the initial burnout rate, which characterizes the rate of loss of fuel weight

181   on the ignition point of the TG curve, f_2 (%) is the late burnout rate, and t_0 (min) is the

182   burnout time, representing the time from the initiation of combustion mass loss to

183   burnout (with a mass loss rate of 98%).

184   The integrated combustion characteristics of the sample are described by

185   combustion index S_N (10^{-12} $K^{-3}min^{-2}$); herein, large values represent better combustion

186   characteristics.

187
$$S_N = \frac{(dw/dt)_{max} \cdot (dw/dt)_{mean}}{t_i^2 t_f}, \qquad (2)$$

188   where $(dw/dt)_{max}$ (%/min) and $(dw/dt)_{mean}$ (%/min) are the maximum and average burn

189   rates, respectively, and t_i (K) and t_b (K) are the ignition and burnout temperatures,

190   respectively.

191   The energy consumption is described by specific energy consumption (*SEC*). The

192   index expresses the energy consumed during densification for unit mass of raw material.

193
$$SEC = \frac{W}{m} = \frac{\int f \cdot ds}{m}, \qquad (3)$$

194   where *SEC* (J/kg) is the specific energy consumption, *W* (J) is densification energy, *m*

195   (kg) is mass of the briquette, and *f* (kN) and *s* (mm) are the pressure and displacement,

196   respectively. In addition, the drop resistance and compaction strength of briquettes were

197   tested according to the method recommended by the China National Standard GB

198   34170-2017 [28].

199   Ozone formation potential (*OFP*) (mg/m^3) was calculated by considering VOC

200   source profiles and maximum incremental reactivity of each species [22].

201
$$OFP = \sum_{i=1}^{n} MIR_i \times VOC_i, \qquad (4)$$

202   where MIR_i and VOC_i represent the maximum incremental reactivity (gram O_3 per gram

203   VOCs) and concentration of the ith VOC species ($\mu g/m^3$).

204 **3. Results and discussion**

205 *3.1 Fuel property*

206 *3.1.1 Basic physicochemical characteristics*

207   As listed in Table 1, the LHV of charcoal was 9.4% higher than that of semi-coke.

208 The addition of charcoal was beneficial for enhancing the heating value of briquettes.

209 The bulk density of charcoal was considerably smaller than that of semi-coke, which

210 had a negative effect on the mass density of briquettes. From the viewpoint of biomass

211 utilization, the energy density was significantly increased by pyrolysis and

212 densification. The atomic H/C and O/C ratio are commonly used to evaluate the energy

213 quality of solid fuels. The smaller the index value, the better the fuel quality for solid

214 fuels [29]. Based on the ultimate analysis results, the atomic O/C ratios of charcoal,

215 semi-coke, and bio-tar were 0.20, 0.31, and 0.51, respectively, whereas H/C ratios were

216 0.02, 0.43, and 0.41, respectively. The O/C and H/C ratios of the charcoal were close

217 to those of anthracite [30], suggesting that the performance of charcoal is better than

218 that of semi-coke. The addition of charcoal and bio-tar negatively affected fuel-N

219 content. The S contents of charcoal and bio-tar were distinctly lower than those of the

220 semi-coke, and therefore, the clean levels of blend fuels are much higher.

221 **Table 1**

222 Characteristics of charcoal, semi-coke, and bio-tar.

Feedstocks	Charcoal	Semi-coke	Bio-tar
Bulk density [kg/m^3]	388	908	/

|				
LHV[a] [MJ/kg]		30.53	27.91	20.51
Proximate analysis [wt%, ad]	Moisture	2.46	7.41	3.07
	Volatile	12.02	9.01	53.57
	Ash	3.35	11.86	9.13
	Fixed carbon	82.03	71.72	34.23
Ultimate analysis [wt%, daf]	C	78.27	68.41	57.32
	H	0.11	2.47	1.97
	O[b]	20.72	28.42	38.68
	N	0.78	0.38	1.93
	S	0.12	0.32	0.10
Metal elements [mg/g]	Na	1.99	2.04	4.33
	K	3.32	0.27	0.79
	Ca	25.52	16.25	5.24
	Mg	22.58	0.52	1.00

223   ad: air-dry basis; daf: dry and ash-free basis.

224   [a] LHV: lower heating value.

225   [b] Calculated by the difference.

226   The thermogravimetry (TG) and differential thermogravimetry (DTG) curves of

227   semi-coke, charcoal, and bio-tar are shown in Fig. 2. The weight losses of the three

228   fuels were clearly different. When the samples were heated, water evaporated, which

229   was accompanied by devolatilization, volatile flaming, and fixed carbon firing. During

230   the first stage with heating temperatures below 100 °C, semi-coke experienced a high

231 reduction in weight owing to the loss of its relatively high moisture content (Table 1).

232 Charcoal exhibited a more intense rate of weight loss during the second stage, and this

233 occurred at a distinctly lower temperature than that of the semi-coke. The curve of bio-

234 tar was the most tortuous, which indicated that the weight loss fluctuated throughout

235 the process owing to its complex components consisting of phenols, amides, and lipids

236 with >20C atoms [31]. The burnout indices and integrated combustion indices of the

237 materials are listed in Table. 2. Bio-tar had the highest reaction rate, whereas charcoal

238 had the lowest ignition and burnout temperatures. The combustion index value depends

239 on the above indices. Charcoal presented the best combustion performance, with

240 burnout and combustion index of 57.41×10^{-4}/min and 36.28×10^{-12} $K^{-3} \cdot min^{-2}$,

241 respectively. Semi-coke showed the poorest combustion performance, with burnout and

242 combustion index of 13.49×10^{-4}/min and 7.73×10^{-12} $K^{-3} \cdot min^{-2}$, respectively. These

243 results highlight the distinctly different combustion characteristics of the three fuels.
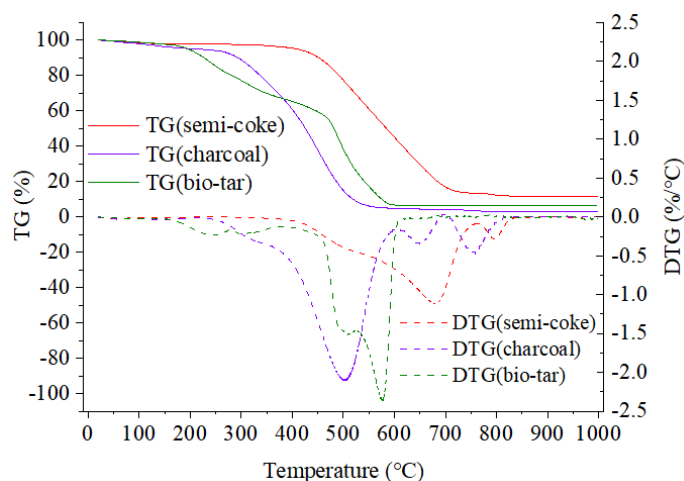
244

245 Fig. 2. Combustion characteristic curves, i.e., thermogravimetry (TG) and differential

246 thermogravimetry (DTG) of charcoal, semi-coke, and bio-tar.

247 *3.1.2 Co-combustion characteristics of charcoal and semi-coke*

248   Blends of charcoal and semi-coke were prepared with mass ratios of 3:7, 5:5, and

249 7:3, which were denoted as CS37, CS55, and CS73, respectively. The TG and DTG

250 curves of CS37, CS55, and CS73 are shown in Fig. 3. With an increase in the proportion

251 of semi-coke, the TG curves of CS73, CS55, and CS37 gradually shifted to the right.

252 This tendency is consistent with the theoretical results. An intense rate of weight loss

253 was achieved for the blends during the second stage than that achieved for semi-coke.

254 Accordingly, the burnout index and integrated combustion index of CS37, CS55, and

255 CS73 increased gradually. A higher burnout index implies lesser time for the fuel to

256 burn out, thereby minimizing unburnt carbon loss [32]. The weighted average values of

257 these indices corresponding to the blending ratio were larger than the test results,

258 suggesting that the interactions occurring between the components of blends slightly

259 lowered the reactivity. The interactive effects varied with the characteristics of

260 components in blends, such as heterogeneity, nature, and distribution of reacting

261 species [33]. However, the integrated combustion index of CS55 reached 16.92×10^{-12}

262 $K^{-3} \cdot min^{-2}$, which was more than two times higher than that of the semi-coke alone,

263 indicating that the blend of charcoal and semi-coke is a promising solid fuel.

264
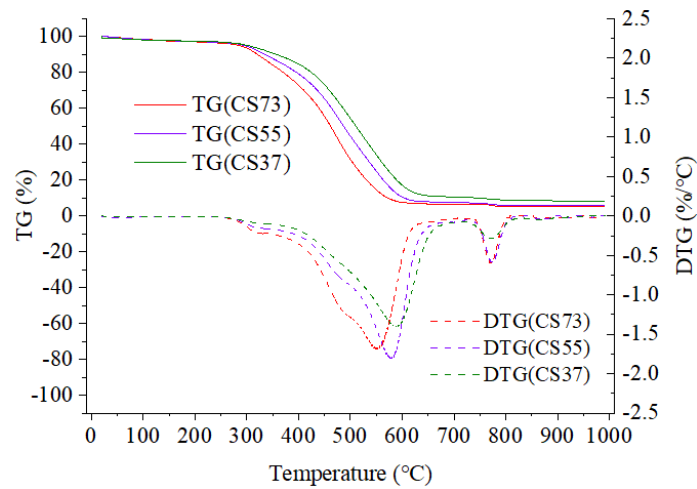
Fig. 3. Co-combustion characteristic curves, i.e., TG and DTG of blends CS37, CS55,

and CS73.

3.1.3 Influence of bio-tar addition on co-combustion characteristics

To analyze the influence of bio-tar addition on the combustion characteristics, 3, 6,

and 9 wt% bio-tar were added to sample CS55, which were denoted as T03, T06, and

T09, respectively. TG and DTG curves of the different blends are shown in Fig. 4.

These curves were almost coincident, indicating that the addition of bio-tar had little

influence on the combustion characteristics of the samples. In fact, the combustion

characteristic parameters of the bio-tar and CS55 were also quite proximate, as shown

in Table 2. The integrated combustion characteristics of T03, T06, and T09 were 14.46–

17.20×10^{-12} $K^{-3}min^{-2}$, which is close to those of CS55. From the viewpoint of

combustion characteristics, the effect of a small amount of bio-tar addition on CS55

could be ignored, suggesting that co-combustion is a feasible method for handling and

using bio-tar.

279
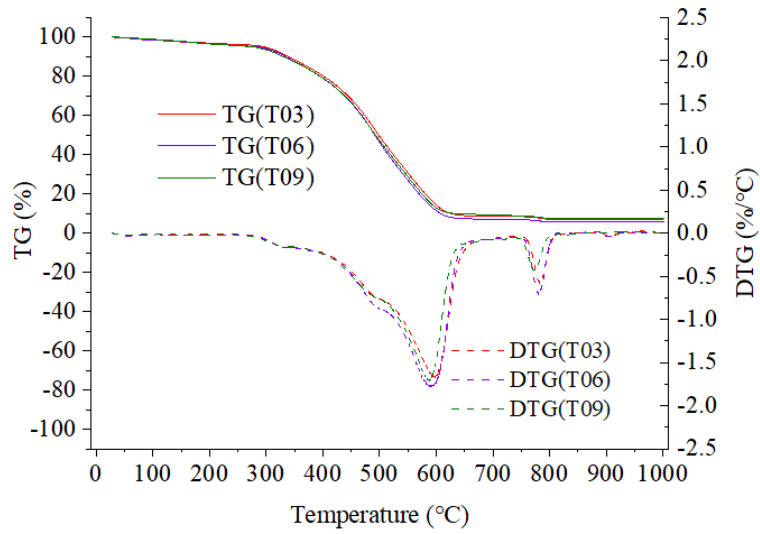
Fig. 4. Co-combustion characteristic curves, i.e., TG and DTG of blends T03, T06,

and T09.

Table 2

Combustion indices of different samples.

Sample	Ignition temperature (°C)	Burnout temperature (°C)	Burnout characteristics C_b/(10^{-4}/min)	Maximum reaction rate $(dw/d\tau)_{max}$/(%/min)	Average reaction rate $(dw/d\tau)_{mean}$/(%/min)	Integrated combustion characteristics S_N/(10^{-12}K^{-3}min^{-2})
Charcoal	349.10	511.80	57.41	-5.53	-4.09	36.28
Semi-coke	415.61	695.65	13.49	-3.23	−2.88	7.73
Bio-tar	391.81	554.94	43.87	−6.31	-3.09	22.87
CS37	405.20	623.15	21.91	-4.03	-3.34	13.15
CS55	382.55	587.09	27.35	-4.25	-3.42	16.92
CS73	380.83	548.72	35.87	-4.95	-3.76	23.37
T03	383.10	598.12	27.69	-3.96	-3.21	14.46
T06	378.30	582.21	29.25	-4.31	-3.32	17.20
T09	368.67	595.96	28.93	-3.93	-3.12	15.15

3.2 Co-densification experiments

Based on the conclusions of co-combustion characteristics detailed in Section 3.1,

a blend with 5:5 mass ratio of charcoal to semi-coke (CK) was selected for further

16

287   analyzing the co-densification characteristics of charcoal and semi-coke using bio-tar

288   as a blinder.

289   *3.2.1 Mechanical strength*

290   In this study, the mechanical strength includes compaction strength and drop

291   resistance, representing the stability of briquettes under the influence of different types

292   of external forces [20][34]. To investigate the influence of densification temperature

293   and bio-tar addition on the mechanical strength of briquettes, densification

294   temperatures of 20, 35, and 50 °C were applied. Briquettes with 3, 6, and 9 wt% bio-

295   tar were prepared and denoted as 3T, 6T, and 9T, respectively. In addition, 1 wt%

296   cellulose was added to the blends as a basic binder for all co-densification experiments.

297   The compaction strength and drop resistance of the charcoal-based briquettes (CK,

298   3T, 6T, and 9T) are shown in Fig. 5. The compaction strength and drop resistance

299   increased distinctly as the proportion of bio-tar addition increased at densification

300   temperatures of 20 and 35 °C. The strength compaction and drop resistance increased

301   by 8.6% and 13.9%, respectively, when the bio-tar addition was increased from 0% to

302   9% at the densification temperature of 20 °C. These results indicate that bio-tar addition

303   had a strong positive effect on densification quality at densification temperatures of 20–

304   35 °C. This trend could be explained by the fact that increasingly more binding

305   compounds are introduced into the briquettes and stronger adhesion bonds of the

306   material particles develop as the proportion of bio-tar addition is increased [10]. SEM

307   images (Fig. S2) with 500× magnification of cross sections show that many

308   interweaving structures of bio-tar and material particles present in T9 densified at

309   temperatures of 20 and 35 °C. The filamentous form of bio-tar and abundant fine

310   charcoal particles embedded in the binders were found, which might effectively

311   strengthen the binding force of the particles. When the temperature was increased to

312   50 °C, the overall mechanical strength was reduced, indicating that increasing the

313   temperature from 20 to 50 °C had an adverse effect on the co-densification performance.

314   The water vapor formed under strong pressure and higher densification temperature

315   might weaken the binding force between the particles [35].
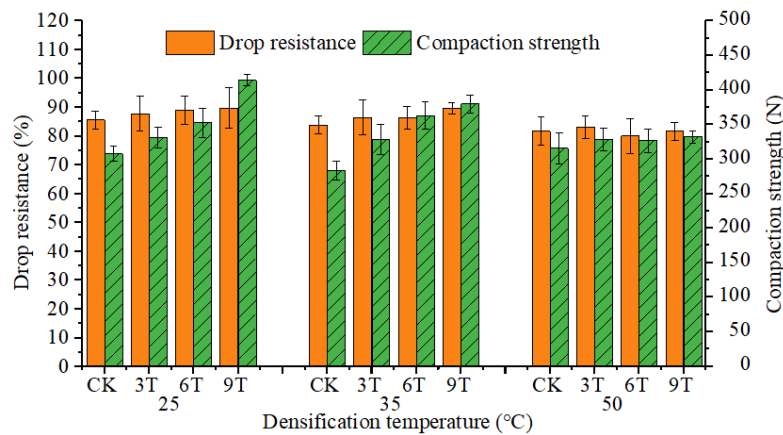

316

317   **Fig. 5.** Compaction strength and drop resistance of charcoal-based briquettes, herein,

318   briquettes with 0, 3, 6, and 9 wt% bio-tar were denoted as CK, 3T, 6T, and 9T.

319   *3.2.2 Energy density and specific energy consumption*

320   Mass density is also an important index of densification quality, as it affects the

321   transportation and use cost of the solid fuels. In general, a higher mass density means a

322   higher energy density for single-material briquettes. The energy density and mass

323   density were not linearly related herein because various proportions of bio-tar were

324 added to the blends, and its heating value was significantly lower than that of charcoal

325 and semi-coke.

326   The mass density, energy density, and specific energy of the charcoal-based

327 briquettes densified under different conditions are shown in Fig. 6. An increase in the

328 proportion of bio-tar addition positively contributed to mass density, and this trend was

329 more obvious at relatively low densification temperatures. Herein, T9 and T6 represent

330 the sample with the largest energy density at the densification temperature of 20 and

331 35 °C. The contribution of bio-tar addition from 6% to 9% to the mass density was

332 insufficient to offset the negative influence of the bio-tar on heating values. Increasing

333 the proportion of bio-tar and densification temperature would help to reduce the SEC.

334 This might be explained as a reduction in friction among the particles and between the

335 particles and die as a result of properly increasing the bio-tar addition and densification

336 temperature [36]. Specific energy affects the production costs; however, the energy

337 consumption of heating the materials at densification temperatures of 35 and 50 °C was

338 not considered herein.
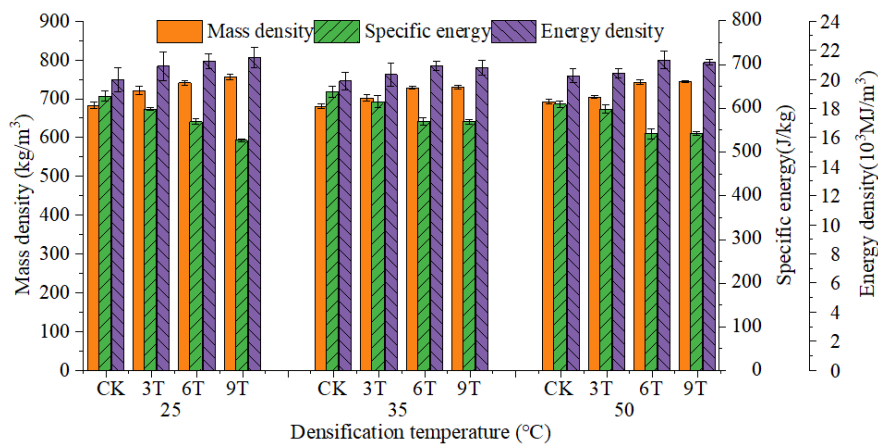
339

340   **Fig. 6.** Energy density and specific energy consumption of various charcoal-based

341   briquettes at different densified temperatures.

342   *3.2.3 Parameter optimization*

343   The effects of bio-tar addition and densification temperature on the compaction

344   strength, drop resistance, mass density, energy density, and specific energy, which

345   represent densification quality and production cost, were investigated. To evaluate the

346   comprehensive performance of different experimental conditions, a gray relation

347   projection, as a comprehensive evaluation method applying the gray system theory and

348   vector projection principle, was adopted herein [37].

349   Based on the index vector (I) shown in equation (5), a decision matrix of gray

350   correlation projection (*Y*) was constructed by combining the test values of each

351   experiment (equation (6)). The first line represents the optimal case of all tests, meaning

352   that the maximum and minimum values were taken for the benefit and cost index,

353   respectively. To eliminate the incommensurability caused by index magnitude and units,

354   the decision matrix (*Y'*) was initialized using percentage conversion (equation (7)). The

355   correlation coefficients between each vector point in space and optimal vector point

356   were calculated, and a gray correlation judgment matrix (*F*) was established as equation

357   (8).

358   I = (*compaction strength*, *drop resistance*, *energy density*, *specific energy*),   (5)

$$Y = \begin{bmatrix} 414.0 & 89.9 & 21499.4 & 526.3 \\ 307.4 & 85.6 & 19965.5 & 627.9 \\ 331.6 & 87.8 & 20890.8 & 598.3 \\ 352.4 & 89.0 & 21252.7 & 569.3 \\ 414.0 & 89.4 & 21499.4 & 526.3 \\ 283.3 & 83.9 & 19874.4 & 637.6 \\ 328.4 & 86.5 & 20327.1 & 614.8 \\ 362.9 & 86.3 & 20904.6 & 570.3 \\ 379.9 & 89.9 & 20776.6 & 568.9 \\ 315.6 & 81.8 & 20244.5 & 609.2 \\ 328.7 & 83.0 & 20396.0 & 598.2 \\ 326.9 & 80.0 & 21311.1 & 541.5 \\ 332.4 & 86.7 & 21153.0 & 542.1 \end{bmatrix}, \quad (6)$$

$$Y' = \begin{bmatrix} 1.00 & 1.00 & 1.00 & 1.00 \\ 0.74 & 0.95 & 0.93 & 0.84 \\ 0.80 & 0.98 & 0.97 & 0.88 \\ 0.85 & 0.99 & 0.99 & 0.92 \\ 1.00 & 0.99 & 1.00 & 1.00 \\ 0.68 & 0.93 & 0.92 & 0.83 \\ 0.79 & 0.96 & 0.95 & 0.86 \\ 0.88 & 0.96 & 0.97 & 0.92 \\ 0.92 & 1.00 & 0.97 & 0.93 \\ 0.76 & 0.91 & 0.94 & 0.86 \\ 0.79 & 0.92 & 0.95 & 0.88 \\ 0.79 & 0.89 & 0.99 & 0.97 \\ 0.80 & 0.91 & 0.98 & 0.97 \end{bmatrix}, \quad (7)$$

$$F = \begin{bmatrix} 1.00 & 1.00 & 1.00 & 1.00 \\ 0.38 & 0.77 & 0.69 & 0.49 \\ 0.44 & 0.87 & 0.85 & 0.57 \\ 0.51 & 0.94 & 0.93 & 0.68 \\ 1.00 & 0.96 & 1.00 & 1.00 \\ 0.33 & 0.70 & 0.68 & 0.47 \\ 0.43 & 0.81 & 0.74 & 0.52 \\ 0.56 & 0.80 & 0.85 & 0.67 \\ 0.66 & 1.00 & 0.82 & 0.68 \\ 0.40 & 0.64 & 0.73 & 0.54 \\ 0.43 & 0.67 & 0.75 & 0.57 \\ 0.43 & 0.59 & 0.95 & 0.85 \\ 0.44 & 0.63 & 0.91 & 0.84 \end{bmatrix}. \quad (8)$$

The weight coefficient vector of each index according to the expert scores was W = (0.13, 0.37, 0.21, 0.29), and the gray correlation projection weight coefficient vector was $W' = (0.03, 0.26, 0.08, 0.16)$. Gray relational projection values (Table 3) of different experimental conditions were obtained based on equation (8) and W'. The larger the

value, the better the comprehensive performance of corresponding briquettes. The best comprehensive performance was achieved with high bio-tar addition under low and medium densification temperatures, average performance was observed with medium and high bio-tar addition at high temperature, and poorest performance was observed at medium and high densification temperatures without bio-tar addition.

Table 3

Gray relational projection values of briquettes under different experimental conditions

Conditions	20 °C	20 °C	20 °C	20 °C	35 °C	35 °C	35 °C	35 °C	50 °C	50 °C	50 °C	50 °C
	CK	3T	6T	9T	CK	3T	6T	9T	CS	3T	6T	9T
Values	0.35	0.40	0.44	0.52	0.32	0.37	0.40	0.46	0.32	0.34	0.38	0.39

3.3 Pollutant emission experiments

Based on the conclusions of co-densification characteristics detailed in Section 3.2, regarding the potential pollutant emission risk of excessive bio-tar addition, charcoal-based briquettes, densified at 20 °C using 6 wt% bio-tar as a binder, were selected to investigate the pollutant emission characteristics. Three samples of briquettes were prepared for a controlled trial study. Herein, CK represents briquettes produced with the blend of charcoal and semi-coke (mass ratio 1:1), 6T represents briquettes produced with 6 wt% bio-tar as a binder based on CK, and 6Tp represents briquettes produced with 3 wt% hydrated lime as a catalyst based on 6T.

3.3.1 Conventional gaseous pollutants

NO$_X$ and SO$_2$ emissions, which are regarded as the main conventional gaseous pollutants, are shown in Fig. 7. NO$_X$ emission concentrations for CK, T6, and T6p were

385 113.2–225.6, 133.1–234.4, and 120.8–208.9 mg/Nm^3, respectively. For these three

386 charcoal-based briquettes, the changing trends in NO$_X$ emissions during different

387 combustion phases were similar, indicating that bio-tar addition had no distinct

388 influence on the NO$_X$ emission. NO$_X$ emissions are mainly affected by the fuel-N

389 content and combustion temperature [38][39]. During the entire process, the stove

390 temperatures showed a trend of initial increase and subsequent decrease for the three

391 briquettes (Fig. S3), and the NO$_X$ emissions varied among different combustion phases.

392 According to the ultimate analysis results in Table. 1, the addition of 6 wt% bio-tar had

393 a little influence on the fuel-N content of the briquettes.

394   The changing trends of SO$_2$ emissions in the three phases were similar. The SO$_2$

395 emission concentrations for CK, T6, and T6p were 22.4–33.1, 20.7–32.6, and 7.8–11.3

396 mg/Nm^3, respectively. In the stable combustion phase, the relatively higher stove

397 temperature resulted in a higher conversion rate of fuel sulfur to gaseous SO$_2$ [40].

398 Overall, the amount of SO$_2$ emission from T6p was significantly lower than that from

399 CK and T6, and the desulfurization efficiency was more than 70%. These results

400 indicate that the addition of hydrated lime was effective for reducing the SO$_2$ emission

401 of charcoal-based briquettes. This can be explained by the fact that $Ca(OH)_2$ can easily

402 capture SO$_2$ and volatile emissions during the combustion process [41].

403

404
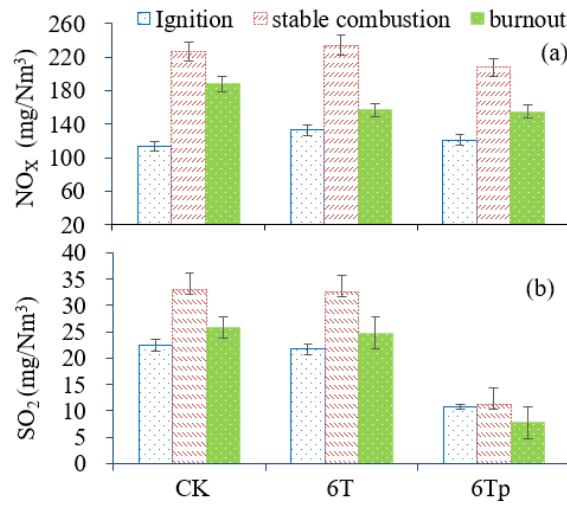
Fig. 7. Emission concentrations of NO_X (a) and SO_2 (b) of CK, 6T, and 6Tp at different

combustion phases (CK, 6T, and 6Tp represent briquettes produced with the blend of

charcoal and semi-coke (mass ratio 1:1), briquettes produced with 6 wt% bio-tar as a

binder based on CK, and briquettes produced with 3 wt% hydrated lime as a catalyst

based on 6T, respectively).

3.3.2 Total suspended particles

The distributions of mean emissions of TSP, including mass size and number size

concentrations, for different briquettes during the entire combustion process are shown

in Fig. 8. The changing trends of the three mass size concentration curves were similar,

indicating that the particle masses were mainly distributed within grades 11–14 with

particle sizes of 2.5–10 μm for the three kinds of briquettes. Meanwhile, the three

number size concentration curves were also similar, indicating that the particle numbers

were mainly distributed within grades 1–7 with particle sizes of <0.16 μm. The mass

and number size of particles within grades 1–7 increased by 2.83 and 2.78 times,

419　respectively, after the addition of bio-tar, whereas after the addition of hydrated lime,

420　these values were significantly reduced by 46.0% and 53.1%, respectively. These

421　results indicate that controlling particulate emission is a key concern for bio-tar addition,

422　and the mechanism of reducing particle emission through the addition of hydrated lime

423　should be further explored [42].
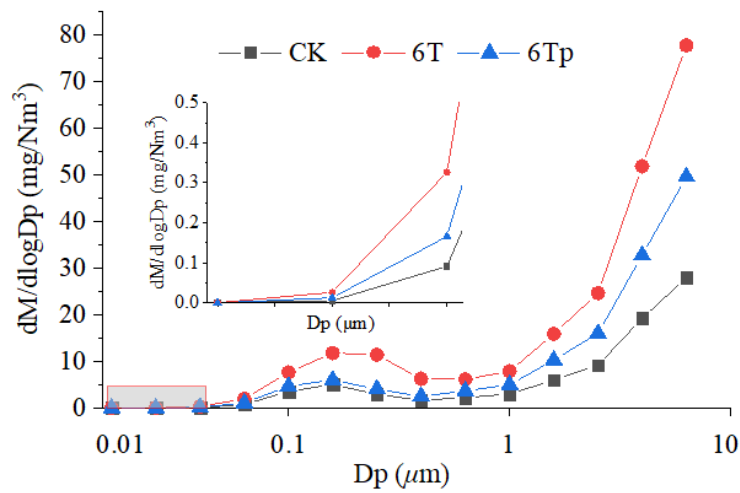
424

425　　　　　　　　　　　　　a. Particle mass size distribution
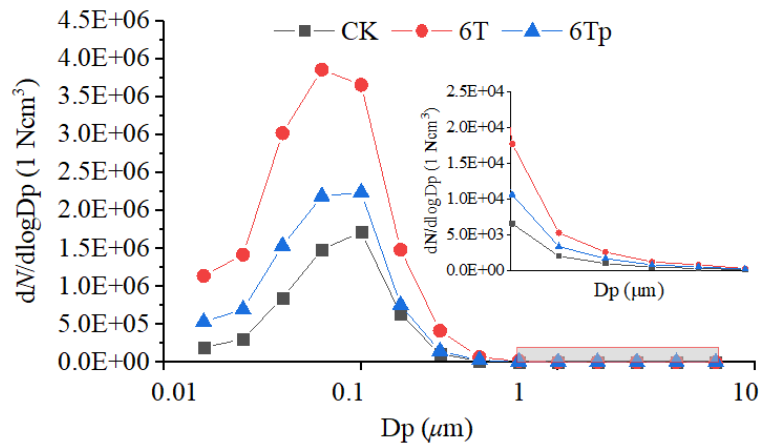
426

427　　　　　　　　　　　　　b. Particle number size distribution

428　**Fig. 8.** Total suspended particles (TSP), mean particle number size, and mean mass

429　size distributions of CK, 6T, and 6Tp throughout the process.

25

The particle concentrations during different combustion phases for CK, 6T, and 6Tp are shown in Fig. 9. The total suspended particles (PM10) and fine suspended particles (PM2.5), which are known to adversely affect the human health, were separately studied. Overall, the concentration of particulate emission during the ignition phase was the largest, regardless of mass size or number size, whereas that in the burnout phase was the smallest. In the three combustion phases, the addition of bio-tar increased the particle emissions, whereas the further addition of hydrated lime significantly decreased it again. Particulate emissions were the highest during the ignition phase, which might be associated with unstable combustion [43]. The bio-tar addition increased the PM10 emission from 12.2 to 33.3 mg/m^3, and then hydrated lime addition decreased it to 21.3 mg/m^3. For PM2.5, the bio-tar addition increased it from 5.1 to 13.8 mg/m^3, and then the further addition of hydrated lime decreased it to 7.6 mg/m^3. These results indicate that the combined addition of bio-tar and hydrated lime is effective for the application of charcoal-based briquettes.


a
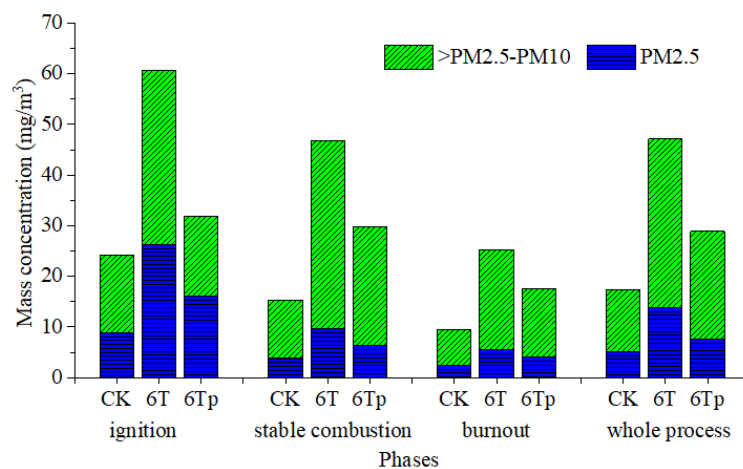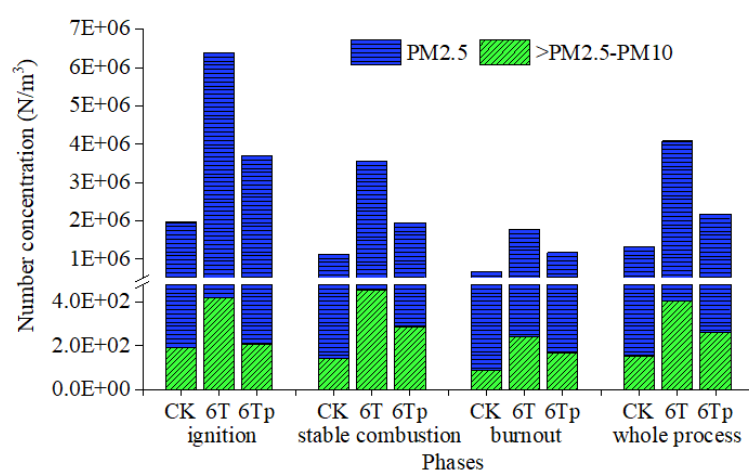
b. Particle number size concentrations

Fig. 9. TSP, particle number size, and mass size concentrations of CS, 6T, and 6Tp

during different combustion phases.

3.3.3 VOCs emission

A total of 98 VOC species were detected using GC/MS according to the China

Environmental Industry Standard HJ 759-2015 [44]. The VOC chemical profiles

emitted from CK, 6T, and 6Tp are shown in Fig. 10. These profiles presented some

similarities, all containing mainly aromatic hydrocarbons, alkanes, and alkenes.

Toluene and m-xylene were the two largest volatile organic pollutants. A small amount

of alkene was detected only for 6T in the ignition and stable combustion phases. This

can be attributed to the presence of an active functional group as an unsaturated bond

that reacts easily with oxygen to form carbon dioxide and water [45].

The concentrations of VOCs fluctuated widely under different experimental

conditions, and these were reflected in the OFP index. The OFP of the CK, 6T, and 6Tp

were 0.18–0.37, 0.24–48.4, and 0.23–37.4 mg/m^3 during the entire combustion process.

462   The bio-tar addition distinctly increased VOC emissions. Comparing 6T with CS, the

463   emission of VOCs increased to 131.3 and 4.5 times during ignition and stable

464   combustion phases, respectively, whereas comparing 6Tp with 6T, VOC emissions

465   decreased to 0.77 and 0.29 times, respectively. The influence of bio-tar addition on

466   VOC emission was the strongest during the ignition phase, but the addition of hydrated

467   lime had only a minor effect. The hydrated lime had a distinct effect during the stable

468   combustion and burnout phases, resulting in similar VOC emissions of 6Tp and CK.

469   This indicates that a higher combustion temperature and hydrated lime addition are key

470   factors for reducing the VOC emission of 6T [46].
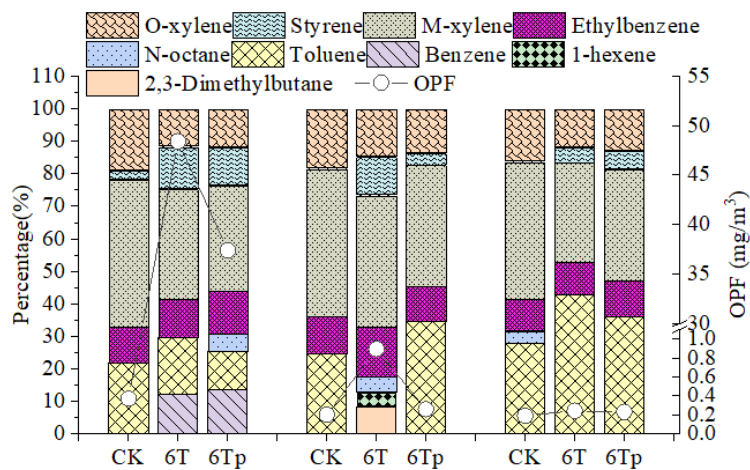
471

472   **Fig. 10.** Mass percentage of VOC species and ozone formation potential for CK, 6T,

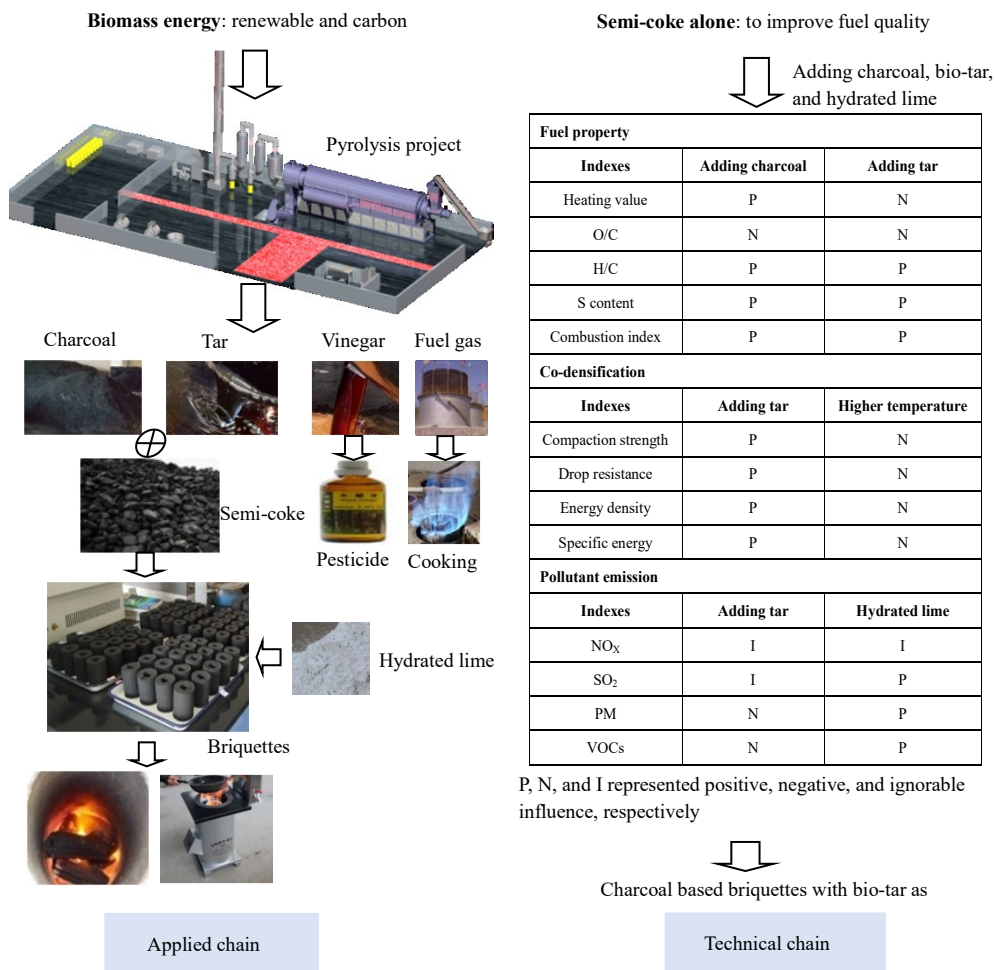473   and 6Tp during different combustion phases.

474   *3.3.4 Comprehensive properties of the briquettes*

475   To utilize charcoal and bio-tar more efficiently and to develop a new heating fuel,

476   a charcoal-based briquette prepared using bio-tar as a binder was investigated

477   systematically from the viewpoint of the fuel properties, co-densification characteristics,

478 and pollutant emission characteristics. The applied chain and technical chain of the

479 charcoal-based briquette are shown in Fig. 11. Regarding fuel properties, the addition

480 of charcoal improved the heating value, S content, atomic ratios of H/C and O/C, and

481 combustion index. There was no distinct influence on the fuel properties, when small

482 amounts of bio-tar were added to the blend CS55. Regarding the co-densification

483 characteristics, the bio-tar addition improved the compaction strength, drop resistance,

484 and specific energy, although some negative effects were observed when the

485 densification temperature was increased from 20 to 50 °C. Regarding the pollutant

486 emission characteristics, the bio-tar addition had a distinctly negative influence on TSP

487 and VOC emissions; however, the adverse influence could be effectively weakened by

488 further adding hydrated lime. Overall, the charcoal-based briquettes prepared with bio-

489 tar as binder are technically feasible.

490 From the viewpoint of application chain, approximately 1.5 billion tons of

491 agroforestry residues are produced annually in China [1]. Some of these resources could

492 be converted to fuel gas, char, bio-tar, and vinegar-like fractions using slow pyrolysis

493 technology. Fuel gas is mainly used as coking energy, and the vinegar-like fraction is

494 purified and used as a pesticide. The remaining char and bio-tar are utilized as heating

495 fuel in rural China with the technical route provided by this investigation. The Chinese

496 government proposed the implementation of projects for clean energy production via

497 biomass pyrolysis technology in the main grain-producing provinces (districts) of North

498 China [47]. Therefore, the promotion and application of new charcoal-based briquettes

are timely and fulfill the actual requirements in China.

Biomass energy: renewable and carbon

Semi-coke alone: to improve fuel quality

Pyrolysis project

Charcoal　Tar　Vinegar　Fuel gas

Semi-coke

Pesticide　Cooking

Hydrated lime

Briquettes

Applied chain

Adding charcoal, bio-tar, and hydrated lime

Fuel property		
Indexes	**Adding charcoal**	**Adding tar**
Heating value	P	N
O/C	N	N
H/C	P	P
S content	P	P
Combustion index	P	P
Co-densification		
Indexes	**Adding tar**	**Higher temperature**
Compaction strength	P	N
Drop resistance	P	N
Energy density	P	N
Specific energy	P	N
Pollutant emission		
Indexes	**Adding tar**	**Hydrated lime**
NO_X	I	I
SO_2	I	P
PM	N	P
VOCs	N	P

P, N, and I represented positive, negative, and ignorable influence, respectively

Charcoal based briquettes with bio-tar as

Technical chain

Fig. 11. Applied chain and technical chain of the charcoal-based briquettes

4. Conclusion

Herein, charcoal-based briquettes prepared using bio-tar as a binder were proposed as a substitute for conventional coal for heating in rural China. The fuel properties of the blends of charcoal, semi-coke, and bio-tar and the co-densification and pollutant emission characteristics of the proposed charcoal-based briquettes were determined. The addition of charcoal improved the heating value and combustion index of the blends. The combustion characteristics of blend CS55 could be improved from 7.73 ×

509   10^{-12} (only semi-coke) to 16.92×10^{-12} $K^{-3}min^{-2}$. The co-densification test indicated that

510   bio-tar could enhance the physical stability of charcoal-based briquettes. The strength

511   compaction and drop resistance increased by 8.6% and 13.9%, respectively, when the

512   bio-tar addition was increased from 0 to 9 wt% at the densification temperature of 20 °C.

513   However, some negative influences were found, when the densification temperature

514   was increased from 20 to 50 °C. Pollutant emissions characteristics were monitored

515   during ignition, stable combustion, and burnout phases of the stove. The bio-tar addition

516   had distinct negative influences, increasing the total suspended particle and VOC

517   emissions. However, this problem was easily overcome by the addition of common

518   additive (hydrated lime) at 3 wt%

519   **Acknowledgements**

525   **References**

526   [1] Cong H, Zhao L, Meng H, Yao Z, Huo L, Jia J, et al. Applicability evaluation of biomass
527   pyrolytic poly-generation technology on clean heating in northern rural of China. Nongye
528   Gongcheng Xuebao/Transactions Chinese Soc Agric Eng 2018;34:8–14.

529   [2] National Energy Administration. Notice on printing winter heating planning (2017-2021)
530   in the northern region (in Chinese). http://www.gov.cn/xinwen/2017-
531   12/20/content_5248855.htm; 2017 [accessed December 20, 2017].

[3]   Ministry of Environmental Protection of the People's Republic of China (MEP). Pollution Comprehensive Management for Residential Coal Combustion (in Chinese). http://www.mep.gov.cn/gkml/hbb/bgg/201610/t20161031_366528.htm; 2016 [Accessed May 21, 2016].

[4]   Guo M, Song W, Buhain J. Bioenergy and biofuels: History, status, and perspective. Renew Sustain Energy Rev 2015. https://doi.org/10.1016/j.rser.2014.10.013.

[5]   Tian J, Ni H, Han Y, Shen Z, Wang Q, Long X, et al. Primary PM2.5 and trace gas emissions from residential coal combustion: assessing semi-coke briquette for emission reduction in the Beijing-Tianjin-Hebei region, China. Atmos Environ 2018;191:378–86. https://doi.org/10.1016/j.atmosenv.2018.07.031.

[6]   Yu J, Paterson N, Blamey J, Millan M. Cellulose, xylan and lignin interactions during pyrolysis of lignocellulosic biomass. Fuel 2017;191:140–9. https://doi.org/10.1016/j.fuel.2016.11.057.

[7]   Sharma HB, Sarmah AK, Dubey B. Hydrothermal carbonization of renewable waste biomass for solid biofuel production: A discussion on process mechanism, the influence of process parameters, environmental performance and fuel properties of hydrochar. Renew Sustain Energy Rev 2020. https://doi.org/10.1016/j.rser.2020.109761.

[8]   Jiang L, Yuan X, Xiao Z, Liang J, Li H, Cao L, et al. A comparative study of biomass pellet and biomass-sludge mixed pellet: Energy input and pellet properties. Energy Convers Manag 2016;126:509–15. https://doi.org/10.1016/j.enconman.2016.08.035.

[9]   Li Q, Li X, Jiang J, Duan L, Ge S, Zhang Q, et al. Semi-coke briquettes: Towards reducing emissions of primary PM 2.5, particulate carbon, and carbon monoxide from household coal combustion in China. Sci Rep 2016; 6. https://doi.org/10.1038/srep19306.

[10] Kang K, Zhu M, Sun G, Qiu L, Guo X, Meda V, et al. Co-densification of Eucommia ulmoides Oliver stem with pyrolysis oil and char for solid biofuel: An optimization and characterization study. Appl Energy 2018;223:347–57. https://doi.org/10.1016/j.apenergy.2018.04.069.

[11] Goldwyn M. The science of charcoal: how charcoal is made and how charcoal works. Pampano Beach, FL: AmazingRibs, Inc. http://www.amazin gribs.com/tips_ and_ technique/zen_of_charcoal.html; 2013.

[12] Cong H, Zhao L, Mašek O, Yao Z, Meng H, Huo L, et al. Evaluating the performance of honeycomb briquettes produced from semi-coke and corn stover char: Co-combustion, emission characteristics, and a value-chain model for rural China. J Clean Prod 2020;244: 1–9. https://doi.org/10.1016/j.jclepro.2019.118770.

566 [13] Shen Y, Wang J, Ge X, Chen M. By-products recycling for syngas cleanup in biomass
567   pyrolysis - An overview. Renew Sustain Energy Rev 2016;1. https://doi.org/
568   10.1016/j.rser.2016.01.077.

569 [14] Sarkar P, Sahu SG, Chakraborty N, Adak AK. Studies on potential utilization of rice husk
570   char in blend with lignite for co-combustion application. J Therm Anal Calorim
571   2014;115:1573–81. https://doi.org/10.1007/s10973-013-3499-z.

572 [15] Liu X, Chen M, Wei Y. Kinetics based on two-stage scheme for co-combustion of
573   herbaceous biomass and bituminous coal. Fuel 2015;143:577–85.
574   https://doi.org/10.1016/j.fuel.2014.11.085.

575 [16] Mundike J, Collard FX, Görgens JF. Co-combustion characteristics of coal with invasive
576   alien plant chars prepared by torrefaction or slow pyrolysis. Fuel 2018;225:62–70.
577   https://doi.org/10.1016/j.fuel.2018.03.024.

578 [17] Cheng J, Zhou F, Si T, Zhou J, Cen K. Mechanical strength and combustion properties of
579   biomass pellets prepared with coal tar residue as a binder. Fuel Process Technol
580   2018;179:229–37. https://doi.org/10.1016/j.fuproc.2018.07.011.

581 [18] Emadi B, Iroba KL, Tabil LG. Effect of polymer plastic binder on mechanical, storage and
582   combustion characteristics of torrefied and pelletized herbaceous biomass. Appl Energy
583   2017;198:312–9. https://doi.org/10.1016/j.apenergy.2016.12.027.

584 [19] Asadullah M, Adi AM, Suhada N, Malek NH, Saringat MI, Azdarpour A. Optimization of
585   palm kernel shell torrefaction to produce energy densified bio-coal. Energy Convers
586   Manag 2014;71. https://doi.org/10.1016/j.enconman.2014.04.071.

587 [20] Kang K, Qiu L, Sun G, Zhu M, Yang X, Yao Y, et al. Co-densification technology as a
588   critical strategy for energy recovery from biomass and other resources - A review. Renew
589   Sustain Energy Rev 2019;12. https://doi.org/10.1016/j.rser.2019.109414.

590 [21] Si T, Cheng J, Zhou F, Zhou J, Cen K. Control of pollutants in the combustion of biomass
591   pellets prepared with coal tar residue as a binder. Fuel 2017;208:439–46.
592   https://doi.org/10.1016/j.fuel.2017.07.051.

593 [22] Carter WPL. Development of ozone reactivity scales for volatile organic compounds. J Air
594   Waste Manag Assoc 1994;44:881–99. https://doi.org/10.1080/1073161x.1994. 10467290.

595 [23] State Administration for Market Regulation, China. Determination of calorific value of
596   coal 2008. http://openstd.samr.gov.cn/bzgk/gb/index.

597 [24] ASTM D5373-16, Standard Test Methods for Determination of Carbon, Hydrogen and
598   Nitrogen in Analysis Samples of Coal and Carbon in Analysis Samples of Coal and Coke,
599   ASTM International, West Conshohocken, PA, 2016, www.astm.org.

[25] ASTM D4239-18e1, Standard Test Method for Sulfur in the Analysis Sample of Coal and Coke Using High-Temperature Tube Furnace Combustion, ASTM International, West Conshohocken, PA, 2018, www.astm.org

[26] AOAC 975.03-1988, Metals in Plants and Pet Foods - Atomic Absorp,1988, http://www.aoacofficialmethod.org/

[27] Moon C, Sung Y, Ahn S, Kim T, Choi G, Kim D. Effect of blending ratio on combustion performance in blends of biomass and coals of different ranks. Exp Therm Fluid Sci 2013;47:232–40. https://doi.org/10.1016/j.expthermflusci.2013.01.019.

[28] State Administration for Market Regulation, China. Commercial coal quality—Civil briquette 2017. http://openstd.samr.gov.cn/bzgk/gb/index.

[29] Van Krevelen D. Graphical statistical method for the study of structure and reaction processes of coal. Fuel 1950;29:269–84.

[30] Uzoejinwa BB, He X, Wang S, El-Fatah Abomohra A, Hu Y, Wang Q. Co-pyrolysis of biomass and waste plastics as a thermochemical conversion technology for high-grade biofuel production: Recent progress and future directions elsewhere worldwide. Energy Convers Manag 2018;2. https://doi.org/10.1016/j.enconman.2018.02.004.

[31] Cong H, Mašek O, Zhao L, Yao Z, Meng H, Hu E, et al. Slow Pyrolysis Performance and Energy Balance of Corn Stover in Continuous Pyrolysis-Based Poly-Generation Systems. Energy Fuel 2018;32:3743–50. https://doi.org/10.1021/acs.energyfuels.7b03175.

[32] Toptas A, Yildirim Y, Duman G, Yanik J. Combustion behavior of different kinds of torrefied biomass and their blends with lignite. Bioresour Technol 2015;177:328–36. https://doi.org/10.1016/j.biortech.2014.11.072.

[33] Sahu SG, Sarkar P, Chakraborty N, Adak AK. Thermogravimetric assessment of combustion characteristics of blends of a coal with different biomass chars. Fuel Process Technol 2010;91:369–78. https://doi.org/10.1016/j.fuproc.2009.12.001.

[34] Adapa P, Tabil L, Schoenau G, Opoku A. Pelleting characteristics of selected biomass with and without steam explosion pretreatment. Int J Agric Biol Eng 2010;3:62–79. https://doi.org/10.3965/j.issn.1934-6344.2010.03.062-079.

[35] Stelte W, Holm JK, Sanadi AR, Barsberg S, Ahrenfeldt J, Henriksen UB. A study of bonding and failure mechanisms in fuel pellets from different biomass resources. Biomass Bioenerg 2011;35:910–18. https://doi.org/10.1016/j.biombioe.2010.11.003.

[36] Tumuluru JS, Wright CT, Hess JR, Kenney KL. A review of biomass densification systems to develop uniform feedstock commodities for bioenergy application. Biofuel Bioprod Bior 2011;11. https://doi.org/10.1002/bbb.324.

634 [37] Zhicai Z, Li C. Analysis on decision-making model of plan evaluation based on grey
635   relation projection and combination weight algorithm. J Syst Eng Electron 2018;36:789–
636   96. https://doi.org/10.21629/JSEE.2018.04.13.

637 [38] Jin Y, Li Y, Liu F. Combustion effects and emission characteristics of SO2, CO, NOx and
638   heavy metals during co-combustion of coal and dewatered sludge. Front Environ Sci Eng
639   2016;10:201–10. https://doi.org/10.1007/s11783-014-0739-9.

640 [39] Roy MM, Corscadden KW. An experimental study of combustion and emissions of
641   biomass briquettes in a domestic wood stove. Appl Energy 2012;99:206–12.
642   https://doi.org/10.1016/j.apenergy.2012.05.003.

643 [40] Zhang S, Jiang X, Lv G, Liu B, Jin Y, Yan J. SO2, NOx, HF, HCl and PCDD/Fs emissions
644   during co-combustion of bituminous coal and pickling sludge in a drop tube furnace. Fuel
645   2016;8. https://doi.org/10.1016/j.fuel.2016.08.061.

646 [41] Qin L, Han J, Mi T, Liu L, Wang H, Yang X. Experimental study on SO$_2$ and NOx removal
647   during briquette combustion. Adv Mater Res 2013;10:634–38.

648 [42] Garcia-Maraver A, Zamorano M, Fernandes U, Rabaçal M, Costa M. Relationship
649   between fuel quality and gaseous and particulate matter emissions in a domestic pellet-
650   fired boiler. Fuel 2014;119:141–52. https://doi.org/10.1016/j.fuel.2013.11.037.

651 [43] Wang J, Lou HH, Yang F, Cheng F. Development and performance evaluation of a clean-
652   burning stove. J Clean Prod 2016;134(B):447–55. https://doi.org/10.1016/j.jclepro.
653   2016.01.068.

654 [44] Ministry of Ecology and Environment of the People's Republic of China. Ambient air-
655   Determination of volatile organic compounds- Collected by specially-prepared canisters
656   and analyzed by gas chromatography/mass spectrometry 2015.
657   http://www.mee.gov.cn/ywgz/fgbz/bz/

658 [45] Cheng J, Zhang Y, Wang T, Xu H, Norris P, Pan WP. Emission of volatile organic
659   compounds (VOCs) during coal combustion at different heating rates. Fuel 2018;225:554–
660   62. https://doi.org/10.1016/j.fuel.2018.03.185.

661 [46] Ma WC, Tai LY, Chen GY, He C, Guan YN, Song GW, et al. Analysis of pollutant
662   emission of typical domestic biomass pellet heating furnaces in Tianjin. Zhongguo
663   Huanjing Kexue/China Environ Sci 2018;38:845–51.

664 [47] National Development and Reform Commission. Guiding on the construction of straw
665   gasification clean energy utilization project (in Chinese).

666 http://www.gov.cn/xinwen/2018-01/02/content_5252602.htm; 2017 [Accessed January 2,

667 2018]

COMPETING INTERESTS

669 The authors declare that they have no competing interests.